Two-Stage Code Acquisition in Wireless Optical CDMA Communications Using Optical Orthogonal Codes

Reza Mirzaei Nejad, Leslie A. Rusch, and Jawad A. Salehi

IEEE Transactions on Communications, (Volume 64, Issue 8) (2016)

Doi: 10.1109/TCOMM.2016.2577685

http://ieeexplore.ieee.org.acces.bibl.ulaval.ca/stamp/stamp.jsp?tp=&arnumber=7486094&isnumber=7542475

Two Stage Code Acquisition in Wireless Optical CDMA Communications using Optical Orthogonal Codes

Reza Mirzaei Nejad, Leslie A. Rusch, *Fellow, IEEE and* J.A. Salehi, *Fellow, IEEE*

***Abstract*— In this paper, we analyze the performance of code acquisition system in atmospheric optical code division multiple access (OCDMA) communications using optical orthogonal codes (OOCs). Memory introduced by temporal correlation of optical fading process precludes us from using Markov chain model for code acquisition analysis. By considering this issue, we discuss how to extend the applicability of Markov chain model to the atmospheric OCDMA communications. We analyze and compare the performance of correlator and chip level detector (CLD) structures in the acquisition system. In our analysis, we consider the effects of free space optical channel impairments, multiple access interference (MAI) and receiver thermal noise in the context of semi-classical photon-counting approach. Furthermore, we evaluate the performance of various two stage schemes that utilize different combinations of active correlator, matched filter (MF) and CLD in search and verification stages, and we find the optimum acquisition scheme among them. Numerical results show significant improvement in reducing the acquisition time and required power for synchronization using our optimum scheme in the wireless OCDMA communications.**

***Index Terms*— Optical code division multiple access (OCDMA), free space optical (FSO), acquisition, Markov chain, correlator, chip level detector (CLD).**

I. Introduction

OVER the past two decades, various optical code division multiple access (OCDMA) techniques have received increasing attention for their potential applications in high speed and high capacity optical access networks. OCDMA via optical orthogonal codes (OOCs) was first introduced for fiber-optic networks using intensity modulation and direct detection (IM/DD) technique [1], [2]. Later, it was employed in IM/DD atmospheric or free space optical (FSO) communications [3]. Atmospheric optical systems can provide high bit rate and cost effective links which also benefit from the security in data transmission and the lack of licensing requirements [4],[5]. Different applications are being investigated for FSO communications [6-8]. A novel idea is a hybrid fiber-optic/FSO OCDMA network which can deliver different multimedia and data services to the users, efficiently and at a low cost. Fig. 1 illustrates a hybrid network with fiber-optic CDMA sub-networks in different locations connected to each other via atmospheric OCDMA links. The free space transmitters and receivers can be mounted on the top of the buildings. By using wireless optical transceivers, different fiber-optic networks are grouped together to form a larger OCDMA network.

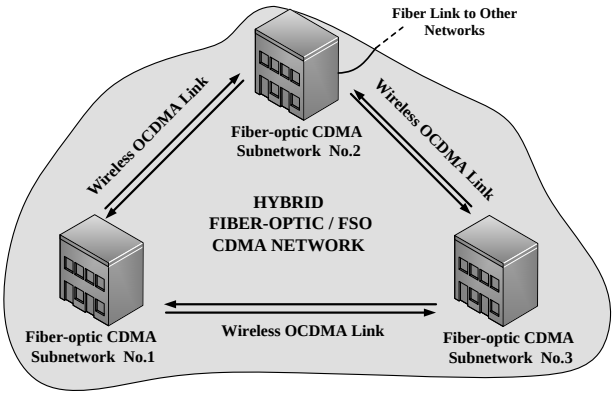

Fig. 1. A hybrid fiber-optic / FSO CDMA network with three fiber-optic CDMA sub-networks connected to each other via wireless OCDMA links

One of the essential requirements to succeed in developing high speed hybrid OCDMA networks is to introduce fast and efficient synchronization systems. The code synchronization system generally consists of an acquisition subsystem that synchronizes the desired receiving code and its locally generated replica in the receiver with a specified accuracy. Then using a tracking circuitry the two codes are precisely synchronized.

In Fig. 1, the code acquisition problem can be studied for fiber-optic sub-networks or the wireless links. For the fiber-optic CDMA sub-networks, after primary studies of OOC acquisition using simulation in [9], [10], single dwell serial search acquisition of OOCs was analyzed in [11] where an

Manuscript received June 1, 2015; revised November 6, 2015, February 25, 2016, and May 2, 2016; accepted May 30, 2016. Date of publication June 7, 2016; date of current version August 12, 2016. Part of this research was supported by Iran National Science Foundation (INSF). The associate editor coordinating the review of this paper and approving it for publication was W. C. Kwong.

Reza Mirzaei Nejad and Leslie A. Rusch are with center for optics, photonics and laser (COPL), Electrical and computer Engineering Department, Laval University, Québec, QC G1V 0A6, (e-mail: reza.mirzaei-nejad.1@ulaval.ca, leslie.rusch@gel.ulaval.ca).

J.A. Salehi is with Electrical Engineering Department, Sharif University of Technology, Tehran, Iran (e-mail: jasalehi@ee.sharif.edu).

active correlator was used as the detector and the effects of multiple access interference (MAI), dark current and shot noise were considered in the analysis. After that, in [12],[13], new acquisition algorithms were discussed in an ideal OCDMA network where an active correlator was used as the detector and only interference effect was considered in signal model. Some variations of [12] were reported in [14], [15] with the same signal and receiver model. In this paper, we focus on the performance analysis of acquisition system in atmospheric OCDMA communications. By using analytical signal model counting for various system impairments, we study the effects of different channel and system parameters on acquisition system performance. Furthermore, we introduce a fast acquisition receiver for wireless OCDMA links of Fig. 1 in a two stage acquisition scheme.

To evaluate the performance of an acquisition scheme, we need to compute the acquisition time using Markov chain model [16]. Turbulence induced fading is the main impairment of the atmospheric channel. Log-normal model [17], [18] is used for the fading of optical wireless channel in our system analysis. We note that the memory introduced by the temporal correlation of fading process precludes us from using Markov chain model to evaluate the performance of the acquisition system [19]. This problem has been studied in radio mobile systems [20-23]; however, no analytical study is available for the atmospheric optical communications in literature. By considering this issue, we discuss how to extend the applicability of Markov chain to the analysis of OOC acquisition in the atmospheric OCDMA communications and present closed form expression for mean of the acquisition time for multiple dwell serial search algorithm. Moreover, we analyze the performance of different detectors including correlator and chip level detector (CLD) [24] in acquisition receiver using the photon-counting approach. In our analysis, we consider all the major sources of error including atmospheric channel impairments, MAI, signal shot noise, receiver thermal noise and dark current and discuss their effects on the acquisition procedure. By evaluating the performance of various two stage acquisition schemes that utilize different combinations of active correlator, passive correlator, i.e. matched filter (MF), and CLD in search and verification stages, we find the optimum scheme among them leading to minimum acquisition time in the atmospheric OCDMA communications.

The proceeding sections of this paper are organized as follows. In section II, system model is described and channel model and synchronization procedure are discussed. In section III, the applicability of Markov chain model to the atmospheric OCDMA communications is discussed. In section IV, probabilities of false alarm and detection of correlator and chip level detector are computed. The numerical results are presented in section V and in section VI, we conclude the paper.

II. System Description

A hybrid OCDMA network is shown in Fig. 2(a). It consists of two fiber-optic sub-networks, each with star configuration, connected to each other via an atmospheric OCDMA link. For simplicity, we illustrated only the transmitter of sub-network No. 1 and the receiver of sub-network No. 2 in the wireless link. Users of the hybrid network may be communicating inside a sub-network or through the wireless link. The signals of the users in sub-network No.1 which are transmitting data to the users in subnetwork No.2 via the wireless channel are all summed together and then sent toward the front end optics of sub-network No. 2 using a free space laser transmitter operating at wavelength λ. For CDMA signaling, OOCs with length F and weight w are used. We use standard OOCs with off-peak auto- and cross correlation bounded by one. On-off keying (OOK) modulation is used by the users. To send a zero or one in a chip time, T_c, an optical pulse with mean photon numbers of $m_0 = 0$ or $m_1 = P_t/h\upsilon$ is used respectively, where P_t is the power of transmitter laser, h is the plank's constant and υ stands for the optical frequency.

We consider the case of data transmission from user i in sub-network No. 1 to user j in sub-network No. 2 through the wireless link. The transmitted signal is impaired by the channel. We denote the transmitted signal by $s_j(t)$ and the impaired received signal by $s_j'(t)$. The subscript j indicates that the transmitted signal was multiplied by OOC code of user j showing the destination of the signal. The received multiple access signal in front end optics of the wireless receiver of sub-network No. 2, denoted by $R(t)$ in Fig. 2(a), will be

$$R(t) = \sum_{k=1}^{N} s_k'(t - \tau_k) \tag{1}$$

where N ($\leq \min(N_1, N_2)$) and τ_k are the number of users transmitting data in the wireless link and the delay associated with the signal transmitted to user k in sub-network No.2, respectively. After passing through the front end optics, the received multiple access signal is sent to all the users of sub-network No.2. The *jth* receiver cannot recover the data sent to it without knowing the value of τ_j. To estimate the value of τ_j, the receiver starts in synchronization mode and the corresponding transmitter starts by sending OOC of user j continuously during the synchronization procedure. Whenever the value of τ_j is estimated, the receiver switches to data recovery mode and the transmitter starts to send data bits. In the next two following subsections, we describe the effects of channel on the transmitted signal and synchronization system structure respectively.

A. Atmospheric Optical Channel

The channel effects on signal propagation can be summarized into attenuation, fading and background light. These parameters vary depending on the weather condition [3-5]. We consider the case of clean and sunny weather. We also assume that pointing error is corrected using front end

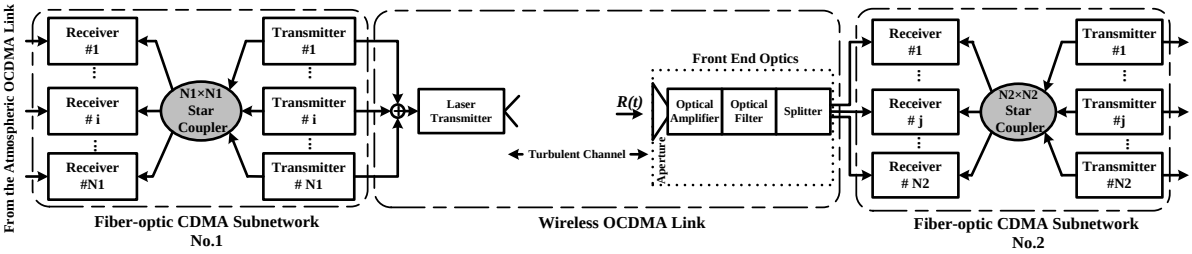

Fig. 2. Structure of a hybrid fiber-optic / FSO CDMA network with two fiber-optic sub-networks connected to each other via wireless optical link.

tracking subsystem [25]. Path gain, a, which counts for attenuation on the signal power caused by absorption and scattering in the channel and also geometrical spreading loss of the transmitted signal, can be computed by [3], [17]

$$a = \frac{A_r}{\pi(\frac{\theta_T L}{2})^2} e^{(-\alpha(\lambda)L)} \tag{2}$$

where A_r, $\alpha(\lambda)$, L and θ are the area of the optical receiver, atmospheric extinction coefficient at wavelength λ, the length of the link and the angle of divergence of transmitter in radians, respectively.

Optical signal fading is caused by random variations of the refractive index along the transmission path in the turbulent channel. It leads the intensity of received signal to fluctuate which results in optical signal fading, also called scintillation in literature [4], [17]. In this paper, we consider low fluctuations of the signal power where the effect of channel on the signal intensity is a multiplicative fading parameter, modeled as a log-normal random variable e^{2x} [17],[18]. Hence, for a transmitted pulse in a chip time with mean photon numbers of m_t, (t = 0, 1), mean photon count of the received pulse, m_r will be

$$m_r = m_t e^{2x} \tag{3}$$

The probability density function (pdf) of x is a normal distribution in the form of $N(-\sigma_x^2, \sigma_x^2)$. Variance of fading, σ_x^2, is computed as $\sigma_x^2 = \min(0.124 k^{\frac{7}{6}} C_n^2 L^{\frac{11}{6}}, 0.5)$ where k=2π/λ, λ, C_n^2 and L are the wave number, wavelength of optical transmitter, refractive index structure constant and the length of the link, respectively. The minimum is taken to simply approximate the saturation of log-normal model [18].

For the background light, the mean number of photons received by the optical receiver in a chip time is

$$m_b = \frac{W(\lambda)\Delta\lambda\, A_r \Omega_{fov} T_c}{h\nu} \tag{4}$$

where W(λ) signifies the spectral radiance function defined as the power radiated at wavelength λ normalized to a cycle of bandwidth in a unit solid angle per unit of source area, Δλ is the front end optical filter bandwidth and Ω_{fov} stands for the receiver field of view in steradian [26].

B. Synchronization in Atmospheric OCDMA Communications

To acquire the code, the uncertainty region of τ_j which is within $[0, FT_c)$ will be divided into F cells of length T_c, each corresponding to a chip shifted version of OOC. For the serial search algorithm, system serially searches different shifts to find the cell (shift) within which the actual value of τ_j is located. In testing each shift, a decision variable is obtained through a correlation process. Then, it is compared with a threshold. The time required to test each shift is called "*dwell time*". Acquisition system can be either single dwell or multiple dwell. In a single dwell acquisition which consists of only a search stage, if the decision variable exceeds the threshold in a shift, that shift is introduced as the correct shift; otherwise it is rejected and the next shift is tested. The decision variable may exceed the threshold in any of the wrong code shifts (named as H_0 cells) or the correct code shift (named as H_1 cell) with the probabilities of false alarm (P_{FAs}) and detection (P_{Ds}), respectively. If a wrong code shift was selected, it takes a considerable time of t_p for the synchronization system to return to the search algorithm and continue the search. t_p is called penalty time.

A more reasonable idea compared to the single dwell acquisition is to use multiple dwell or two stage acquisition consisting of search and verification stages. We use two stage acquisition structures in our receiver, as depicted in Fig. 2(b). In a two stage acquisition scheme, after a decision variable exceeds the threshold in a code shift in search stage, system goes to verification stage where using a verification strategy, it tests the accepted shift again. The aim of using a verification stage is to ensure that the correct shift was selected in the search stage. Despite the radio CMDA systems using pseudo noise (PN) codes where partial correlation with different lengths of PN code is being used in different dwells of verification [27], we have to use full code length correlation in verification stage due to the properties of OOCs [11]. We use majority verification with full length correlation over a bit time. The use of algorithms such as multiple bit observation which can give diversity gain will not lead to a better

performance because our system is line of sight and there is only one path between the laser of transmitter and aperture of receiver in our system. In majority verification, the selected shift is tested for A times. If in at least B tests out of A tests, the decision variable exceeds the threshold, the acquisition is confirmed. We can define probabilities for false alarm (P_{FAv}) and detection (P_{Dv}) in verification stage as well, which mean to confirm a wrong shift or the correct shift, respectively. The detectors used in the two stages can be different. We evaluate the performance of all combinations of the three different detectors of active correlator, MF and CLD in search and verification stages of our acquisition receiver to find the one leading to minimum acquisition time in wireless OCDMA communications. We will describe their structures and compute their P_{FA} and P_{D} in atmospheric channel in section IV.

To evaluate and compare the performance of different acquisition receivers, we need to compute the time required to acquire the code, denoted by T_{Acq}. Since T_{Acq} is a random variable, its statistical characteristics must be considered in the performance evaluation. In the next section, we use Markov chain model and obtain a closed form expression for mean of T_{Acq} of multiple dwell serial search algorithm in atmospheric OCDMA communications.

III. Analysis of Acquisition Algorithm using Markov Chain Model

In this section, we model the acquisition procedure as a discrete Markov chain and we obtain a closed form expression for the mean of acquisition time, E(T_{Acq}). Markov diagram of the serial search algorithm is illustrated in Fig. 3(a). We consider one sample per chip. Although considering more than one sample per chip results in to system performance improvement, but in this theoretical study, we consider one sample per chip to make the interference signal modeling tractable. The conclusions of this paper won't be affected by this assumption. Therefore, each node in the diagram corresponds to a chip-shifted version of locally generated OOC. Without loss of generality, we assume the *Fth* shift to be the correct shift in the diagram. In the two stage serial search acquisition, gain of a typical branch connecting two nodes of *i* and *i+1*, depicted in Fig. 3(b), for i = 1, 2, …, *F*-1, can be computed as

$$H(\mathrm{z}) = H_{nFA}(\mathrm{z}) + H_{FA}(\mathrm{z})\,H_{p}(\mathrm{z}) = [1-P_{FAs}]\,z^{t_s} + [P_{FAs}(1-P_{FAv})]\,z^{t_s+t_v} + [P_{FAs}P_{FAv}]\,z^{t_s+t_v+t_p} \tag{5}$$

where P_{FAs} and t_s are the probability of false alarm and dwell time in search stage, respectively. The dwell time of system must be one bit duration (T_{b}) for active correlator and CLD or one chip duration (T_c) for passive correlator in order to obtain all the pulses of OOC. t_{v} is the time required for the verification. Since majority verification is used, the verification time equals to At_s. P_{FAv} is the probability of confirming a wrong code shift in the verification stage which can be computed as

$$P_{FAv} = \sum_{t=B}^{A} \binom{A}{t} \left(P_{FAv,1}\right)^{t} \left(1-P_{FAv,1}\right)^{A-t} \tag{6}$$

where $P_{\mathrm{FAv,1}}$ is the probability of false alarm in one single test in the verification stage. t_{v} is the time required for the verification. Since majority verification is used, the verification time equals to AT_s.

Two other gain of branches in the diagram of Fig. 3(a) are $H_{\mathrm{D}}(\mathrm{z})$ and $H_{\mathrm{M}}(\mathrm{z})$, corresponding to detection and miss-detection of the correct shift, respectively. They are expressed as

$$H_D(z) = P_{Ds}P_{Dv}z^{t_s+t_v} \tag{7}$$

$$H_M(z) = [1-P_{Ds}]\,z^{t_s} + P_{Ds}[1-P_{Dv}]\,z^{t_s+t_v} \tag{8}$$

P_{Ds} and P_{Dv} are the probability of detecting the correct shift in search mode and confirming the detection of correct shift in the verification mode, respectively; P_{Dv} can be computed as

$$P_{Dv} = \sum_{t=B}^{A} \binom{A}{t} \left(P_{Dv,1}\right)^{t} \left(1-P_{Dv,1}\right)^{A-t} \tag{9}$$

where $P_{\mathrm{Dv,1}}$ is the probability of detection in one single test in the verification mode. The relations (5), (7), (8) can be also used for single dwell serial search, by omitting those terms associated with the verification stage.

If we assume the search starts from each shift randomly with the same probability of 1/F and follow the same approach as presented in [6]-[7], we can obtain the mean of the acquisition time, E(T_{Acq}), as

$$E\left(T_{acq}\right) = \frac{1}{H_D(1)}\left[H_D'(1) + H_M'(1) + (F-1)H'(1).\left(1-\frac{H_D(1)}{2}\right)\right] \tag{10}$$

where the prime marks stand for derivative of expressions with respect to z.

To extend the applicability of the Markov chain model to the atmospheric OCDMA communications, we should consider that the basic assumption for modeling the acquisition procedure as a discrete Markov chain is that the decision variables in different code shifts must be statistically independent [19]. In wireless optical links, temporal correlation of fading process introduces a memory to the system, leading to statistical dependence of fading samples inside a temporal span identified by the coherence time of fading process (T_{f}). Since the decision variables are related to the fading level, depending on the value of T_{f} compared to dwell time (t_s), the decision variables in consecutive code shifts may become correlated. This fact makes it impossible to model the acquisition procedure as a Markov chain in a fading

channel with arbitrary coherence time. However, we can consider two extreme cases, for which, we can still use this analytical tool:

Case I, $T_f < t_s$: in this case, fading level, *x*, changes independently from testing a shift to another. Thus the statistics of different code shifts are independent.

Case II, $T_f >> E(T_{Acq})_{min}$: In this case, fading level changes very slowly and can be assumed to be constant during the acquisition procedure. In fact, fading acts similar to an attenuating factor which is constant during the acquisition procedure but it takes a random value every time the code is acquired. In this case, all the decision variables are completely correlated and they are all (a) ed on the same fading level.

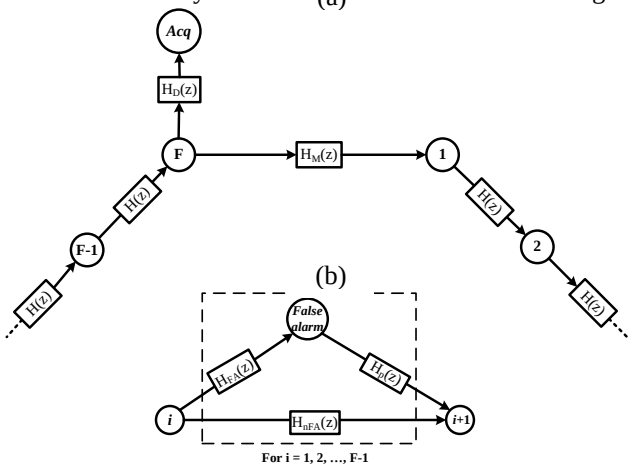

Fig. 3. (a) Markov chain diagram of two stage serial search acquisition algorithm. (b) A typical branch connecting two nodes of *i* and *i+1*

$E(T_{Acq})_{min}$ is the minimum required time to acquire the code using an algorithm. One can simply obtain it by setting P_D=1 and P_{FA}=0.

In case I, we can directly use the Markov chain model. First we average the probability functions of P_D and P_{FA} with respect to fading; next, we use them in gain of branches in (5),(7),(8) and finally we should do the algebra in (10) to obtain the mean of acquisition time, $E(T_{Acq})$. For case II, it is not possible to use the Markov chain model directly because different decision variables are completely correlated. To model the acquisition procedure as a Markov chain in this case, the decision variables and gain of branches in (5), (7), (8) must be modified to be conditioned on the fading level. Conditioned on the fading level, the decision variables become independent. Afterwards, we can compute the mean of acquisition time conditioned on fading level, $E(T_{Acq}|x)$.

For the atmospheric optical channel under log-normal fading, coherence time of fading process is on the order of several milliseconds [17], [18]. On the other side, wireless optical links are usually designated for high bit rate communications. $E(T_{Acq})_{min}$ which is depended on bit duration, equals to $Ft_s/2$ and $Ft_s/2+t_v$ for the single dwell and multiple dwell serial search algorithms, respectively. By assuming the bit rate is sufficiently high and then comparing the two parameters of T_f and $E(T_{Acq})_{min}$, we approximate the channel to be static from acquisition point of view and apply the approach presented for case II to analyze the acquisition algorithm. In the numerical results section, we verify the accuracy of our analysis via simulating the performance of acquisition system. By modifying the gain of branches to be conditioned on fading level and doing the algebra, we compute $E(T_{Acq}|x)$ for multiple dwell serial search algorithm as

$$E\left(T_{Acq}|x\right)=\frac{1}{P(D\mid x)}\Big[\, t_s\left(1+P\left(DF|x\right)\right)+\, t_v\left(P\left(D_s|x\right)+P\left(FA_s|x\right)P\left(DF|x\right)\right)+\, t_p\left(P\left(FA|x\right)P\left(DF|x\right)\right)\Big] \tag{11}$$

where $P(D|x)$, $P(FA|x)$, and $P(DF|x)$ are defined as

$$P\left(FA|x\right)=P\left(FA_s|x\right)P\left(FA_v|x\right) \tag{12}$$

$$P\left(D|x\right)=P\left(D_s|x\right)P\left(D_v|x\right) \tag{13}$$

$$P\left(DF|x\right)=\left(F-1\right)\left(1-\frac{P\left(D_s|x\right)P\left(D_v|x\right)}{2}\right) \tag{14}$$

Finally, to obtain $E(T_{Acq})$, we need to average $E(T_{Acq}|x)$ with respect to the fading level

$$E\left(T_{Acq}\right)=E_x\left(E(T_{Acq}\mid x)\right)=\int_{-\infty}^{+\infty}E(T_{Acq}\mid x)\,f\left(x\right)dx \tag{15}$$

where *f(x)* is the pdf of fading level. To evaluate the mean of acquisition time, P_{FA} and P_D conditioned on fading level must be computed. In the next section, we compute them for the correlator and CLD structures.

IV. Computing P_{FA} and P_D for Detectors

In this section, we compute P_{FA} and P_D for the correlator and chip level detector. The expressions, derived here, can be regarded as the probabilities for the search mode (P ($FA_s|x$), P ($D_s|x$)) or a single test of the verification mode (P ($FA_{v,1}|x$), P ($D_{v,1}|x$)). As aforementioned in (1), each user in sub-network No.2 receives signals of *N* transmitters. We first focus on the signal received from one interfering user, $s_k'(t)$. Then, we discuss on the received multiple access signal, denoted by $R(t)$ in (1). The effect of fading, background light, thermal noise, shot noise and dark current are considered in our analysis. Photon count of each of *w* marked chips of the received signal has a Laguerre distribution [26]. We use notation of *lag(a, b, D)* for the Laguerre distribution with mean ($m_{lag}(a, b, D)$) and variance ($var_{lag}(a,b, D)$) of $a+Db$ and $a+D(b+b^2)+2ab$, respectively. The received signal is first amplified using an erbium doped fiber amplifier (EDFA), with gain *G* and noise factor $K=n_{sp}$ $(G-1)$, where n_{sp} is spontaneous emission parameter. Next, it is photodetected using a PIN photodetector with quantum efficiency of η. Laguerre distribution can preserve its form after optical amplification

and photodetection [18].

If a pulse with the mean photon numbers of m_1 is sent in *ith* marked chip (i=1, 2, …, w), the distribution of its photo-electron count after amplification and photo-detection in the receiver is expressed as [18],[26]

$$lag\left(\eta G m_s e^{2x},\ \frac{\eta}{N_2}\left(G\left(\frac{m_b}{D_t}\right)+K\right),\ D_t\right) \tag{16}$$

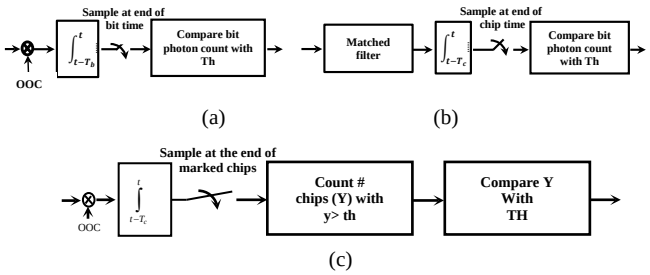

Fig. 4. Three different detectors for search and verification stages of the acquisition receiver. (a) Active correlator. (b) MF. (c) CLD

where e^{2x} and D_t correspond to intensity fading factor and the number of background light temporal modes in a chip time, respectively. We define m_s as am_1/N_2 and D_t equals to $2B_0T_c$ where B_0 is the bandwidth of filter used in front end optics [26]. After photo-detection, dark current of photodetector and thermal noise current of receiver are also added to the received signal. Dark current leads to a Poisson electron count in a chip time, with mean and variance of $m_d=i_DT_c/e$ where i_D is photodetector dark current and e is the electron charge. Thermal noise contributes to each chip, a zero mean Gaussian electron count with variance of $\sigma_{th}^2 = 2K_bT_rT_c/\left(Re^2\right)$, where K_b, T_r and R are Boltzman's constant, receiver equivalent temperature and load resistance, respectively. Electron count of a maked chip is the summation of these three independent currents. We approximate its distribution conditioned on fading level by a Gaussian distribution. Due to the dominance of thermal noise, this method is considered to be accurate [3],[18]. Since the three currents are independent, mean and variance of electron count in each of w marked chips (i = 1,2, …, w) are expressed as

$$m_i = m_{lag}\left(\eta G m_s e^{2x},\ \frac{\eta}{N_2}\left(G\left(\frac{m_b}{D_t}\right)+K\right),\ D_t\right)+m_d \tag{17. a}$$

$$\sigma_i^2 = var_{lag}\left(\eta G m_s e^{2x},\ \frac{\eta}{N_2}\left(G\left(\frac{m_b}{D_t}\right)+K\right),\ D_t\right)+m_d+\sigma_{th}^2 \tag{17. b}$$

where m_{lag} and var_{lag} are the mean and variance of Laguerre distribution.

To consider all multiple access received signals, we use chip synchronous assumption for all interfering users meaning that the delays of all interfering users in (1) are integer multiples of chip time. In [1], it is shown that the chip synchronous assumption, which simplifies the mathematical modeling of interference, leads to an upper bound for the performance of the OCDMA systems when compared to chip asynchronous case. For our analytical expressions for $E(T_{Acq})$ to be the upper bound with respect to interference, we should consider the worst case for the delay of desired user resulting in lowest P_D. Therefore, we cannot apply the chip synchronous assumption to the delay of desired user because it is the best case possible. Instead, we assume its delay to be odd multiple of half chip time, so that its effect is minimized in the receiver and even in the correct shift position, we obtain 1/2 pulse from it in each of marked chips. Photo-detected multiple access signal is used by the detector structure in the receiver for decision making.

A. Correlator

The structures of active and passive correlators are depicted in Fig. 4(a)-(b). The performance of passive correlator which is a MF is the same as active correlator meaning that all the expressions derived here for P_{FA} and P_D can be used for both structures; however, MF benefits from rapidity and can compute the correlation in a chip time duration compared to a bit time in the active correlator. We prefer to explain the analysis of the performance of correlator considering the active structure. In the active correlator structure, the received signal from photodetector is multiplied by the shift of OOC under test; Then the output of multiplier is integrated over a bit time duration and the result is compared with a predefined threshold. We note that multiplying the received signal with different code shifts in the active correlator is equivalent to changing the sampling chip in MF.

Based on the cross correlation property of the OOCs, a chip synchronized interfering user can contribute at most one pulse in one of the marked chips of locally generated OOC [2]. Hence, the effect of an interfering user can be described by (17). In addition, the desired user, based on the autocorrelation property of the OOCs, can contribute at most one pulse in one of marked chips in wrong code shifts (H_0 cells). In fact, in all wrong code shifts, it functions similar to the interfering users. Therefore, we have N similar interfering users in all wrong shifts. When a wrong shift of locally generated code is being tested, the mean and variance of photon count received in *hth* marked chip (h=1,2,...,w), is computed as

$$m_h = m_{lag}\left(l_h\eta G m_s e^{2x},\ \frac{\eta}{N_2}\left(G\left(\frac{m_b}{D_t}\right)+K\right),\ D_t\right)+m_d \tag{18.a}$$

$$\sigma_h^2 = var_{lag}\left(l_h\eta G m_s e^{2x},\ \frac{\eta}{N_2}\left(G\left(\frac{m_b}{D_t}\right)+K\right),\ D_t\right)+ m_d+\sigma_{th}^2 \tag{18.b}$$

where l_h is the number of interfering users in *hth* marked chip. Since the photon counts of different chips are independent and fading level is considered to be constant in a dwell time as discussed in section III, the mean and variance of decision variable in wrong code shifts will be

$$m_{FA} = \sum_{h=1}^{w} m_h = \; l\;\eta G m_s e^{2x} + \frac{\eta}{N_2} w G m_b + \frac{\eta}{N_2} w D_t K + w m_d \quad (19.\text{a})$$

$$\sigma_{FA}^2 = \sum_{h=1}^{w} \sigma_h^2 = \; m_{FA} + w D_t \left[\frac{\eta}{N_2} \left(G\left(\frac{m_b}{D_t} \right) + K \right) \right]^2 + 2\left(\eta l G m_s e^{2x} \right) \left(\frac{\eta}{N_2} \left(G\left(\frac{m_b}{D_t} \right) + K \right) \right) + w\sigma_{th}^2 \quad (19.\text{b})$$

where $l = \sum_{h=1}^{w} l_h$, is the number of interfering users in that shift. The probability of false alarm conditioned on interference and fading equals to

$$P(FA \mid l, x) \;=\; pr\,(\, n \geq Th \mid l,\; x,\; H_0)$$
$$= \int_{Th}^{\infty} \frac{1}{\sqrt{2\pi\sigma_{FA}^2}}\, \mathrm{e}^{-\frac{(\mathrm{n}-m_{FA})^2}{2\sigma_{FA}^2}}\, \mathrm{dn} \;=\; Q\left(\frac{Th - m_{FA}}{\sigma_{FA}} \right) \quad (20)$$

where n and Th are the decision variable and threshold of correlator, respectively, and Q(x) equals to $\int_x^{\infty} \frac{1}{\sqrt{2\pi}} e^{-\frac{t^2}{2}} dt$. In the correct shift ($H_1$ cell), the desired user contributes 1/2 pulse to any of the marked chips of locally generated OOC and it is interfered with signals of N-1 other users. Assuming l_D interfering users in the correct shift, (19) can be used for the mean (m_D) and variance (σ_D^2) of the decision variable in the correct shift by substituting l by (l_D+$w/2$). The probability of detection conditioned on interference and fading, then equals to

$$P(D \mid l_D, x) \;=\; pr\,(\, n \geq Th \mid l_D,\; x,\; H_1) \;=\; Q\left(\frac{Th - m_D}{\sigma_D} \right) \quad (21)$$

Next, we average the probability functions with respect to interference. In [1], it is shown that for the chip synchronous case and OOK modulation, l can be approximated by a binomial distribution defined

$$l \sim Binomial\left(N, \frac{w^2}{2F} \right) \quad (22)$$

By averaging (20) with respect to interference, P_{FA} conditioned on fading level is

$$P\left(FA|x\right) = E_l\left(\, P\left(FA|l,x\right)\right) =$$
$$= \sum_{l=0}^{N} \binom{N}{l} \left(\frac{w^2}{2F} \right)^l \left(1 - \frac{w^2}{2F} \right)^{N-l} \; P\left(FA|l,x\right) \quad (23)$$

We can obtain $P(D|x)$ in a similar fashion to (22) by averaging (20) with respect to l_{D}

$$P\left(D|x\right) = E_{l_D}\left(\, P\left(D|l_D,x\right)\right) =$$
$$\sum_{l_D=0}^{N-1} \binom{N-1}{l_D} \left(\frac{w^2}{2F} \right)^{l_D} \left(1 - \frac{w^2}{2F} \right)^{N-1-l_D} \; P\left(D|l_D,x\right) \quad (24)$$

B. Chip level Detector

The structure of CLD is depicted in Fig. 4(c). In a CLD, the photo-detected multiple access signal is multiplied by the shift of OOC under test. Then an integration process is conducted on each marked chip separately. Chip electron count variable (y) is compared with a chip threshold (th) resulting to a primary decision on its value. If $y>th$, chip is detected as one, otherwise it is detected as zero. To make the final decision, number of chips detected as one (Y) is counted and compared with the bit threshold (TH). If $Y>TH$, that shift is accepted as the correct shift, otherwise it is rejected and system continues the search with the next shift. Although the optimum value for TH in fiber-optic channel is the code weight [24], we modify TH to a smaller value which is proved to be effective in performance improvement in turbulent channel [3]. To derive the expressions for probabilities of false alarm and detection, using the idea presented in [3], we define lower and upper bounds for them. For the lower bound, we assume that if a chip is interfered, it is interfered with only one user and upper bound is defined by assuming that when a chip is interfered, it is certainly detected as "one". To compute lower and upper bound of P_{FA} and P_D, we make them conditioned on the number of chips in the receiver which are interfered by the received multiple access signal. This approach is valid in the case where the number of interfering users is less than the code weight. We define P_0 and P_1 as the probabilities of event ($y>th$), in H_0 cells, when a marked chip is interfered with zero or one user, respectively. P_0 and P_1 can be computed with the mean and variance of (18) by substituting l_h with c

$$m_c = \; c\eta G m_s e^{2x} + \frac{\eta}{N_2} G m_b + \frac{\eta}{N_2} D_t K + m_d \,, c = 0,1 \quad (25.\text{a})$$

$$\sigma_c^2 = m_c + D_t \left[\frac{\eta}{N_2} \left(G\left(\frac{m_b}{D_t} \right) + K \right) \right]^2 + 2\left(c\eta G m_s e^{2x} \right) \left(\frac{\eta}{N_2} \left(G\left(\frac{m_b}{D_t} \right) + K \right) \right) + \sigma_{th}^2 \,, c = 0,1 \quad (25.\text{b})$$

$$P_c = \; pr\left(y > th \mid x,\; H_0 \right) = Q\left(\frac{th - m_c}{\sigma_c} \right), \quad c = 0,1 \quad (26)$$

We further define P_2 and P_3 to be the probabilities of event ($y>th$) in the correct shift position when a chip is interfered with zero and one user, respectively. The mean and variance of chip decision variable in the correct shift position can be computed using (25) by substituting c with (c-3/2) for c =2, 3. P_2 and P_3 are computed as

$$P_c = pr\left(y > th \mid x,\ H_1\right) = Q\left(\frac{th - m_c}{\sigma_c}\right),\ \ c = 2,3 \tag{27}$$

In testing a H_0 cell, if the number of chips detected as one, exceeds *TH*, false alar2[]\m occurs. These chips can be among the interfered or non-interfered chips. If we assume that *l* users have interfered in *r* chips out of *w* chips, lower bound for P_{FA} is obtained as follows

$$P_L(FA|l,\ r,x) = pr\left(Y > TH \mid l,\ r,x,\ H_0\right) = \sum_{j=0}^{r} \sum_{k=\max(TH-j,0)}^{w-r} \binom{w-r}{k}\binom{r}{j} P_0^{\,k}\left(1-P_0\right)^{w-r-k}\ P_1^{\,j}\left(1-P_1\right)^{r-j} \tag{28}$$

To explain (28), we assume *j* interfered chips are detected as one. If $j < TH$, then for false alarm to happen, at least *TH-j* chips among non-interfered chips should be detected as one. For $j > TH$, the number of chips detected as one from non-interfered chips can be any value from zero to *w-r*. For the upper bound, all the interfered chips are assumed to be detected as one. Thus, for the upper bound we have

$$P_U\left(FA\,|l,r,x\right) = pr(Y > TH \mid l,\ r,x,\ H_0) = \sum_{k=\max(TH-r,0)}^{w-r} \binom{w-r}{k} P_0^{\,k}\left(1-P_0\right)^{w-r-k} \tag{29}$$

Lower and upper bound of P_D can be computed in a similar fashion to P_{FA}, using (28), (29) by substituting P_0 and P_1 with P_2 and P_3, respectively.

In the next step, we should average the probability functions with respect to the number of interfered chips. By averaging with respect to *r*, lower bound of P_{FA} is expressed as

$$P_L\left(FA|l,x\right) = \sum_{r=1}^{\min(l,w)} \frac{\binom{w}{r}\binom{l-1}{r-1}}{\binom{w+l-1}{w-1}}\ P_L\left(FA|l,r,x\right) \tag{30}$$

The other probability functions can be obtained exactly the same way as (30), substituting $P_L(FA|l,r,x)$ with one of the other desired probabilities of $P_U(FA|l,r,x)$, $P_L(D|l_D,r,x)$ and $P_U(D|l_D, r, x)$.

Finally, we should average the probability functions with respect to the number of interfering users. For false alarm we have

$$P_L(\mathrm{FA} \mid \mathrm{x}) = \sum_{l=1}^{N} \binom{N}{l}\left(\frac{w^2}{2F}\right)^{l}\left(1-\frac{w^2}{2F}\right)^{N-l} P_L\left(FA|l,x\right) + P_{FA0} \tag{31}$$

Upper bound can be simply computed substituting $P_L(FA|x)$ with $P_U(FA|x)$ in (31). P_{FA0} is P_{FA} for r=0 and l=0. Since there is no interfering user, then there is no difference between lower and upper bound of P_{FA0}

$$P_{FA0} = P\left(FA \mid l = 0, x\right) = \left[1-\frac{w^2}{2F}\right]^{N} \sum_{j=th}^{w} \binom{w}{j} P_0^{\,j}\left(1-P_0\right)^{w-j} \tag{32}$$

Similary, the probability of detection conditioned on fading is obtained as

$$P_L(D \mid x) = \sum_{l_D=1}^{N-1} \binom{N-1}{l_D}\left(\frac{w^2}{2F}\right)^{l_D}\left(1-\frac{w^2}{2F}\right)^{N-1-l_D} P_L(D \mid l_D, x) + P_{D0} \tag{33}$$

for which, P_{D0} is computed as

$$P_{D0} = P\left(D|l_D = 0, x\right) = \left[1-\left(\frac{w^2}{2F}\right)\right]^{N-1} \sum_{j=th}^{w} \binom{w}{j} P_2^{\,j}\left(1-P_2\right)^{w-j} \tag{34}$$

The upper bound of probability of detection can be computed from (33) by substituting $P_{\mathrm{L}}(D|l,x)$ with $P_{\mathrm{U}}(D|l,x)$.

Since $E(T_{\mathrm{Acq}}|x)$ is expressed in terms of P_{FA} and P_{D}, defining lower and upper bounds for these two probability functions, results in lower and upper bounds for $\mathrm{E}(T_{\mathrm{Acq}}|\mathrm{x})$. The lower bound of $\mathrm{E}(T_{\mathrm{Acq}}|\mathrm{x})$ is obtained by using $P_{\mathrm{L}}(FA|x)$ and $P_{\mathrm{U}}(D|x)$ and the upper bound is obtained by using $P_{\mathrm{U}}(FA|x)$ and $P_{\mathrm{L}}(D|x)$.

V. Numerical Results

In this section, we present numerical results for the effect of various impairments on acquisition procedure and discuss on the performance of different acquisition schemes. System parameters and their corresponding values are listed in Table I. We introduce two new parameters named as the mean number of acquisition bits, $\mathrm{E}(N_{\mathrm{Acq}})$, and normalized threshold, (*Nth*). $\mathrm{E}(N_{\mathrm{Acq}})$ is defined as the mean acquisition time divided by bit time. Nth is defined for the correlator structure as

$$Nth = \frac{th - w\eta G m_b - w m_d - \eta w D_t K}{G\eta w m_s} \tag{35}$$

It can be modified to be used as *Nth* for a chip in CLD by substituting *w* with 1.

In Fig. 5, we simulated the performance of acquisition system in fading channel and compared the results with those obtained from analytical expressions to verify the accuracy of approach we discussed in section III. A code set of F= 500, w= 7 is used for two subnetworks with 5 and 6 users where 5 pair of users are active in FSO link. For the simulation, the coherence time of the channel is set to 2*ms*. To generate correlated log-normal random variables for our simulations, we used the approach presented in [28]. We used single dwell acquisition scheme with the active correlator as the detector. $\mathrm{E}(N_{\mathrm{Acq}})$ is plotted versus *Nth*. Simulation results are compared to the analytical expressions of two extreme cases of (I) completely correlated fading statistics in different code shifts where the fading level over all the acquisition procedure is

constant and (II) independent fading statistics in different code shifts where fading level changes from testing a shift to another. The curves corresponding to these two extreme cases are denoted by "corr fading" and "ind fading" in figure, respectively.

The comparison between the simulation and analytical results is done at bitrate of 100 Mbps. Although wireless optical channels are designed for higher bitrates [5], this bit rate is chosen to study the validity of our analytical expressions for a wide range of bitrates selected by network designers. The expressions given in section III are based on the comparison between $E(T_{Acq})_{min}$ and coherence time where we argued that coherence time is much larger than $E(T_{Acq})_{min}$. Based on that, we assumed that fading level is constant over the whole acquisition procedure. Lower bitrate results in to a larger $E(T_{Acq})_{min}$. Coherence time can be on the order of several milliseconds where we have set it to 2ms. A low bit rate and a small coherence time in our simulation will let us examine how accurate our assumption of "constant fading level over acquisition time" is. It is obvious that if our analytical expressions predict the performance correctly for 100 Mbps, they can surely predict the performance for higher bitrates. We observe excellent agreement between the results obtained from the analytical expression associated with the completely correlated fading statistics and the simulation results which validates the assumption we made in section III in our analytical approach. By comparing the minimum of $E(N_{Acq})$ for the two cases of correlated and uncorrelated optical fading statistics during the acquisition procedure, we observe that correlated fading statistics results into increase of acquisition time. This increase of acquisition time becomes more significant in larger variances of fading.

For any set of values of system parameters, there is an optimum threshold where $E(N_{Acq})$ is minimum. For example, in variance of fading of 0.5, based on curves corresponding to simulations and "cor fading", the optimum *Nth* should be set around 0.05. If we wrongly use the expressions for "ind fading" to analyze the performance, then optimum *Nth* will be around 0.09. We observe if the correlated optical fading statistics is not considered in system analysis, it results in wrong threshold setting using the corresponding analysis. By comparing the simulation curve for the two *Nth* of 0.05 and 0.09, we observe a large increase in the acquisition time by using the wrong optimum *Nth*. This fact emphasizes the importance of considering the effect of correlated fading statistics in threshold setting in acquisition system analysis. We also emphasize that threshold setting should be sufficiently accurate for OOC-OCDMA systems otherwise it results into a penalty in acquisition time.

In Fig. 6, the performance of active correlator and CLD, as the detector in a single dwell acquisition receiver, is evaluated and compared. $E(N_{Acq})$ is plotted versus *Nth* in fading variances of 0, 0.1, 0.2 and 0.5. In Fig. 6(a), we considered a fading variance of zero and discussed the effects of thermal noise, EDFA and background light on acquisition procedure. Ideal cases, where thermal noise and background light are set to zero with no pre amplification being used, are plotted as baselines. We observe that by using an optical preamplifier with proper gain, we can suppress the thermal noise effect on acquisition procedure (lines with circle marker) and achieve values for $E(N_{Acq})$ very close to ideal case of shot noise limited. For the system parameters of Table I, gain of 20 dB is sufficient to overcome the thermal noise effect. The difference between $E(N_{Acq})$ of these lines with the ideal cases is mostly due to the spontaneous emission noise of EDFA. The performance of two detectors, by considering the optimum thresholds, are almost the same in a zero fading channel; However, if the amplifier cannot give us enough gain (lines with cross marker, G=10 dB), the performance of CLD degrades more than correlator. We also investigate the case of high background light photon count (lines with triangle marker) which can be due to the presence of other light sources or reflection of surrounding buildings in the field of view of the receiver. We observe that the performance of correlator degrades more compared to CLD in a high background noise environment. It can impose almost the same penalty levels to the acquisition time in the correlator structure as an insufficient amplifier gain. This emphasizes a careful design and locating for the front end optics of the receivers.

In Fig. 6(b), the effect of fading is also included. The performance of detectors deteriorate with increase in the variance of fading. By considering the optimum thresholds and comparing $E(N_{Acq})$ of the two detectors in the same variance of fading, we observe that CLD outperforms

TABLE I
Nominal values used for Numerical Results

λ	wavelength	1.55μm
L	length of the link	3 km
R_b	bit rate	100 Mbps
$\Delta\lambda$	optical filter bandwidth	8nm
i_d	photodetector dark current	10 nA
$W(\lambda)$	spectral radiance function	$10^{-3}\frac{w}{cm^2 \mu m\, sr}$
θ_{FOV}	field of view	10 mRad
A_r	area of aperture	47cm^2
P_t	Transmitted power	12 mW
α	atmospheric extinction coefficient	0.3 km^{-1}
Θ_T	Angle of divergence	1mrad
m_s	mean photon numbers in a transmitted pulse normalized to number of receivers and path gain	100
η	quantum efficiency	0.8
R	load resistance	100 ohm
n_{sp}	spontaneous emission parameter	1.7
A, B	verification parameters	4,2
t_p	penalty time	2 μs
T_r	receiver temperature	300 K
G	EDFA gain	20 dB

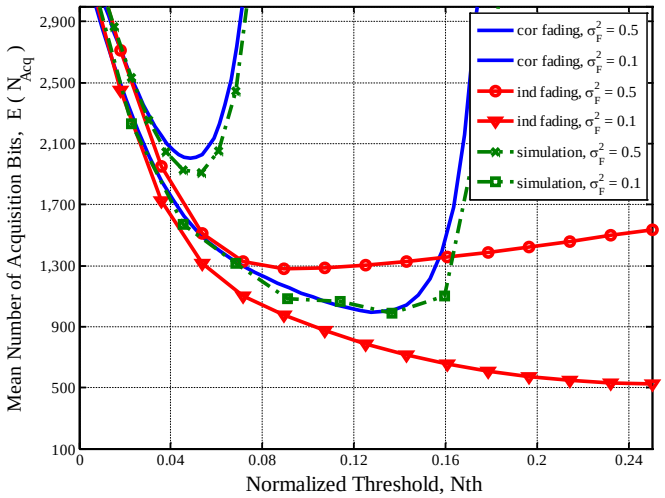

Fig. 5. Comparison of the results obtained from simulation and analytical expressions; E(N_{Acq}) versus normalized threshold

correlator. Therefore, we conclude that CLD has a better performance than correlator as the detector in the acquisition system of free space systems even though it is more sensitive to amplifier gain fluctuation. Since the optimum range of *Nth* changes for different variances of fading, we use the thresholds optimum for the strongest fading ($\sigma_F^2 = 0.5$) in receivers. Based on this idea, we should set *Nth* of the correlator and CLD in fading channel around 0.05 and 0.03, respectively. These thresholds are not optimum for smaller variances of fading, but the degradation in performance using these thresholds is nearly negligible when compared to the case of using the optimum threshold of smaller variances of fading. We also ran simulations with two samples per chip and compared it with the analytical results to show the penalty using analysis with one sample per chip. Simulation results are shown by curves with dashed lines. As can be observed, using two samples per chip, the acquisition time decreases but more importantly the comparison between the performance of CLD and correlator which is the main discussion in this figure doesn't change where CLD always outperforms correlator.

In Fig. 7, the performance of various two stage acquisition schemes which utilize different combinations of active correlator, MF and CLD in search and verification stages is evaluated. E(N_{Acq}) is plotted versus variance of fading. E(N_{Acq}) of single dwell scheme using active correlator is also plotted for comparison. We observe that the performance of single dwell active correlator which is the acquisition scheme formerly used in [11-13] is worse than all the two stage acquisition schemes. The superiority of the performance of the two stage schemes is due to their false alarm avoidance capability. We should note that the optimum threshold for $\sigma_F^2 = 0.5$ is used in the detectors. Under such a circumstance, E(N_{Acq}), for small variances of fading, is not necessarily smaller than that of larger variances in the correlator structure. That is the reason for E(N_{Acq}) of the curves to decrease with the increase of fading variance in low turbulence. The active/active scheme which is the scheme using active correlator in both stages of search and verification

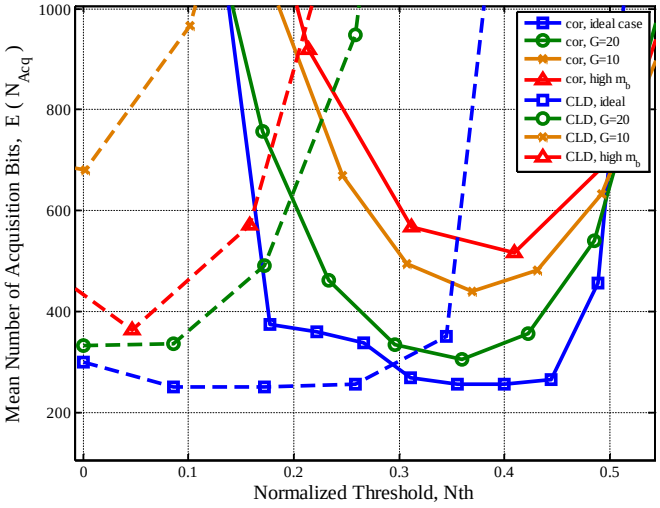

(a)

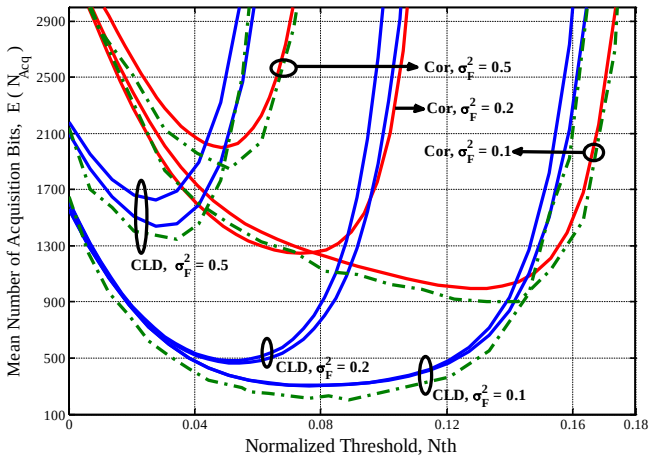

(b)

Fig. 6. Comparison of E (N_{Acq}) of correlator and CLD in a single dwell acquisition scheme (a) In a non-turbulent channel, $\sigma_F^2 = 0$. (b) In fading channel with $\sigma_F^2 = 0.1, 0.2, 0.5$

stages has the worst performance between two stage acquisition schemes. Next two stage scheme is MF/Active which uses MF in search mode and active correlator in the verification mode. We observe that it has better performance than active/active scheme as a result of the rapidity of the MF. The performance of MF/MF which is a detector using MF in search and verification is the same as MF/Active. These two schemes differ in verification detector, where MF and active correlator result in the same P_{FA} and P_D and their dwell time in verification stage is also the same. The next scheme is CLD/CLD which has better performance compared to the two former two stage schemes due to superiority of the performance of CLD to the correlator. The last acquisition scheme is MF/CLD which takes advantage of the rapidity of MF in search mode and superior performance of CLD in the verification mode. We observe that its performance is a little worse than CLD/CLD in very small variances of fading, but in larger variances of fading, it has much better performance compared to the CLD/CLD. Other combinations of the correlator and CLD can be analytically deduced to have worse

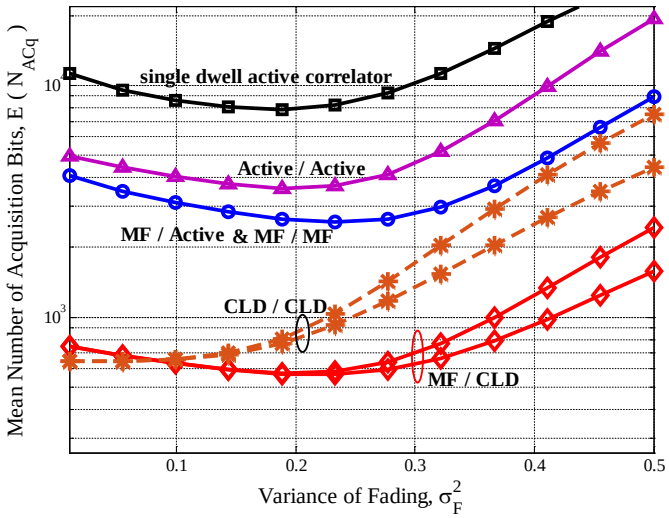

Fig. 7. Comparison of performances of single dwell active correlator and various two stage acquisition schemes in fading channel; E(N_{Acq}) versus variance of fading

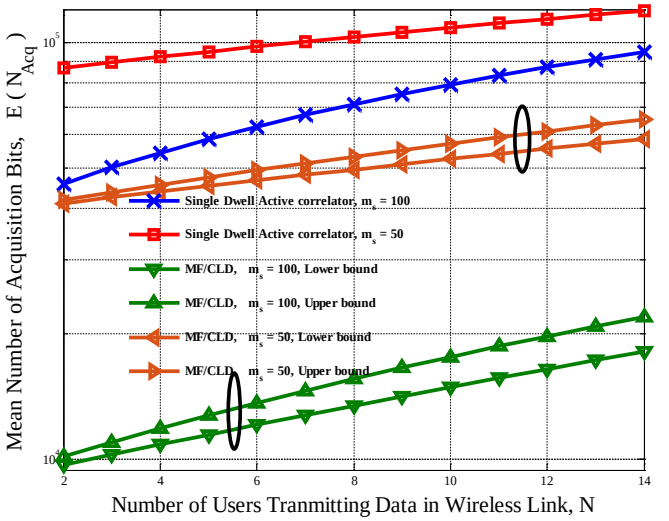

Fig. 8. Effect of number of interfering users in wireless link on E(N_{Acq}) for m_s= 50, 100; comparison of single dwell using active correlator and MF/CLD

performance than MF/CLD and we do not discuss them in Fig. 7. For example, the performance of CLD/Active is certainly worse than CLD/CLD because they differ in verification detector where CLD outperforms active correlator. Therefore, we introduce MF/CLD as the optimum two stage acquisition scheme for fading channel among all the possible combinations of correlator and CLD.

In Fig. 8, E (N_{Acq}) is plotted versus the number of users communicating through the wireless link. We compare the performance of our optimum MF/CLD scheme found in Fig.7 and single dwell scheme using active correlator that was already used in [11-13] as the acquisition receiver, for mean number of transmitted photons of 50 and 100. An OOC set with F=6500 and w=15 is used in a hybrid network with two fiber-optic sub-networks, each with 15 users. To study the performance of acquisition schemes in terms of E(N_{Acq}) versus number of users in the network and transmitted power, we set the variance of fading to 0.5. The acquisition time increases with the increase in the number of users communicating through the wireless link. By comparing the performance of two acquisition schemes, we observe that for an increased number of users, the superiority of MF/CLD to the single dwell active correlator becomes more significant which is mostly due to the MAI resistance of CLD detector. For low transmitted power (m_s=50), the performance of acquisition system degrades and E(N_{Acq}) increases. By comparing the two acquisition schemes, we observe that by using MF/CLD, we achieve the same E(N_{Acq}) as the single dwell active correlator scheme with less than half of the transmitted power.

VI. Concluding Remarks

In this paper, we discussed how to extend the applicability of Markov chain model to the acquisition algorithm analysis in the atmospheric OCDMA communications. It enabled us to analytically evaluate the performance of the code acquisition system in optical fading channel. We validated our approach by comparing the analytical results with those obtained from simulation. We analyzed the performance of correlator and chip level detector in acquisition system. By discussing the effects of different parameters such as fading and background light on the acquisition procedure, we showed that CLD outperforms correlator. Furthermore, we evaluated the performance of various two stage acquisition receivers employing different combinations of active correlator, MF and CLD in search and verification stages and showed that MF/CLD structure outperforms all the other combinations of these three detectors. Numerical results show significant reduction in the acquisition time and the required transmitted power for synchronization in the atmospheric OCDMA communications by using our proposed MF/CLD structure instead of formerly used active correlator structure.

Acknowledgment

The Authors would like to thank Dr. M. Jazayerifar for his constructive criticism and helpful comments.

References

[1] J. A. Salehi, “Code-division multiple-access techniques in optical fiber networks—Part I: Fundamental principles,” *IEEE Trans. Commun*, vol. 38, no. 8, pp. 824–833, Aug. 1989.

[2] J. A. Salehi and C. A. Brackett, “Code division multiple-access techniques in optical fiber networks—Part II: System performance analysis,” *IEEE Trans. Commun.*, vol. 37, no.8 pp. 834–842, Aug. 1989.

[3] M. Jazayerifar and J. A. Salehi, " Atmospheric Optical CDMA Communication Systems via Optical Orthogonal Codes,"*IEEE Trans. Commun*, vol. 54, no. 9, pp 1614–1623, Sep. 2006.

[4]Advanced Optical Wireless Communication Systems, Cambridge: Cambridge University Press, 2012.

[5] M. Kavehrad, M.I. S. Chowdhury, Z. Zhou, “Short Range Optical Wireless : Theory and Applications,” Wiley, 2015.

[6] N. Iliev and I. Paprotny, “Review and Comparison of Spatial Localization Methods for Low-Power Wireless Sensor Networks,” *IEEE Sensors Journal*, vol. 15, no. 10, pp 5971-5987, Oct. 2015.

[7] A. Sharma R.S. Kaler, “Designing of high-speed inter-building connectivity by free space optical link with radio frequency backup,” IET Commun., Vol. 6, Iss. 16, pp. 2568–2574, 2012.

[8] A. Kaadan, H. H. Refai, and P. G. LoPresti, “Multielement FSO transceivers alignment for inter-UAV communications,” *J. Lightwave Tech.*, vol. 32, no. 24, pp 4785-4795 , Dec 15, 2014.

[9] M. M. Mustapha and R. F. Ormondroyd, “Performance of a serial-search synchronizer for fiber-based optical CDMA systems in the presence of

multi-user interference," *Proc. SPIE*, vol. 3899, pp. 297–306, Nov. 1999.
[10] ____, "Dual-threshold sequential detection code synchronization for an optical CDMA network in presence of multi-user interference," *J. Lightwave Technol.*, vol. 18, pp. 1742–1748, Dec. 2000.
[11] A. Keshavarzian and J. A. Salehi, "Optical orthogonal code acquisition in fiber-optic CDMA systems via the simple serial-search method," *IEEE Trans. Commun.*, vol. 50, no. 3, pp. 473–483, Mar. 2002.
[12] A. Keshavarzian and J. A. Salehi, "Multiple-shift code acquisition of optical orthogonal codes in optical CDMA systems," *IEEE Trans. Commun.*, vol. 53, no. 4, pp. 687–697, Apr. 2005.
[13] Benedetto, F.; Giunta, G., "On efficient code acquisition of optical orthogonal codes in optical CDMA systems," *IEEE Trans. Commun.*, vol. 58, no. 2, pp. 438–441, Feb. 2010.
[14] J. I. Park, J. Lee, and S. Yoon "An Optical Orthogonal Code Acquisition Scheme for Optical CDMA Systems," APCC 2012.
[15] D. Chong, Y. Joung, S. Yoon', S. Y. Kim, "An Improved Multiple-Shift Algorithm for Rapid Code Acquisition in Optical CDMA Systems," ICACT 2007.
[16] A. Polydoros and C. L. Weber, "A unified approach to serial search spread-spectrum code acquisition—Part I: General theory," *IEEE Trans.Commun.*, vol. COM-32, pp. 542–549, May 1984.
[17] L. C. Andrews and R. L. Philips, Laser Beam Propagation Through Random Media, Washington, D.C.: SPIE Optical Engineering Press, 2005.
[18] M. Razavi and J. H. Shapiro, "Wireless optical communications via diversity reception and optical preamplification," *IEEE Trans. Wireless Commun.*, vol. 4, no. 3, pp. 975–983, May 2005.
[19] G. E. Corazza, C. Caini, A. Vanelli-Coralli, and A. Polydoros, "DS-CDMA code acquisition in the presence of correlated fading—Part I:Theoretical aspects," *IEEE Trans. Commun.*, vol. 52, no.7, pp. 1160–1168, Jul 2004.
[20] Carlo Caini, Giovanni E. Corazza, and Alessandro Vanelli-Coralli, "DS-CDMA code acquisition in the presence of correlated fading—Part II: Application to Cellular Networks," *IEEE Trans. Commun.*, vol. 52, no.7, pp. 1160–1168, Jul 2004.
[21] Henri Puska, Jari Iinatti, and Harri Saarnisaari, "serial search and maximum selection based code acquisition techniques for single and multi antenna systems," *IEEE Trans. Commun.*, vol.8, no.5, pp.2317-2327, May 2009.
[22] Gaetano Giunta, Francesco Benedetto, "Spread-Spectrum Code Acquisition in the Presence of Cell Correlation," *IEEE Trans. Commun*, vol. 55, no. 2, Feb. 2007.
[23] Wern-Ho Sheen et al., "Effects of cell correlations in a matched-filter PN code acquisition for direct-sequence spread-spectrum systems Wern-Ho Sheen," *IEEE Trans. Veh. Technol.*, vol.48, no.3, pp. 724-732, May 1999.
[24] H. M. H. Shalaby, "Chip-level detection in optical code-division multiple-access," *J. Lightw. Technol.*, vol.16, no.6, pp. 1077–1087, Jun 1998.
[25] M. Matsumoto, K.Osawa, S.Hotta, K.Wakamori, "Innovative Tracking System for Next Generation FSO systems under Massive Earthquakes," ONDM, 2015.
[26] R. M. Gagliardi and S. Karp, *Optical Communication*, 2nd ed. New York: Wiley, 1995.
[27] Seung Hwan Won and Lajos Hanzo, "Initial Synchronization of Wideband and UWB Direct SequenceSystems: Single – and Multiple-Antenna Aided Solutions," *IEEE Comm. Surveys & Tutorials*, vol. 14, no. 1, first quarter 2012.
[28] Frederick M. Bomse, "Generation of correlated log-normal sequences for the simulation of clutter echoes," *professional paper 323*, CNA Corporation, Dec. 1981.

Reza Mirzaei Nejad was born in Rasht, Iran in 1985. He received his B.Sc. and M.Sc. degrees both in electrical engineering in 2008 and 2011, respectively. He is currently working toward his Ph.D. degree in center for optics, photonics and laser (COPL) in ECE department of Université Laval, Canada. His research interests mainly include digital signal processing for optical communication systems, mode division multiplexing systems and optical access networks.

Leslie Ann Rusch (S'91-M'94-SM'00-F'10) received the B.S.E.E. degree (with honors) from the California Institute of Technology, Pasadena, in 1980 and the M.A. and Ph.D. degrees in electrical engineering from Princeton University, Princeton, NJ, in 1992 and 1994, respectively. Dr. Rusch has experience in defense, industrial and academic communications research. She was a communications project engineer for the Department of Defense from 1980-1990. While on leave from Université Laval, she spent two years (2001-2002) at Intel Corporation creating and managing a group researching new wireless technologies. She holds a Canada Research chair in Communications Systems Enabling the Cloud and a full professor in the ECE department at Université Laval, QC, Canada, performing research on wireless and optical communications. She is a member of the Centre for Optics, Photonics, and Lasers (COPL) at Université Laval.

Prof. Rusch's research interests include digital signal processing for coherent detection in optical communications, spatial multiplexing using orbital angular momentum modes in fiber, radio over fiber and OFDM for passive optical networks; and in wireless communications, optimization of the optical/wireless interface in emerging cloud based computing networks, and implantable medical sensors with high bit rate UWB telemetry. She is recipient of the IEEE Canada J. M. Ham Award for Graduate Supervision. Prof. Rusch has published over 126 journal articles in international journals (90% IEEE/IEE) with wide readership, and contributed to over 165 conferences. Her articles have been cited over 4300 times per Google Scholar.

Jawad A. Salehi (M'84-SM'07-FM'10) was born in Kazemain, Iraq, on December 22, 1956. He received the B.Sc. degree from the University of California, Irvine, in 1979, and the M.Sc. and Ph.D. degrees from the University of Southern California (USC), Los Angeles, in 1980 and 1984, respectively, all in electrical engineering. He is currently a Full Professor at the Optical Networks Research Laboratory (ONRL), Department of Electrical Engineering, Sharif University of Technology (SUT), Tehran, Iran. From 1981 to 1984, he was a Full-Time Research Assistant at the Communication Science Institute, USC. From 1984 to 1993, he was a Member of Technical Staff of the Applied Research Area, Bell Communications Research (Bellcore), Morristown, NJ. Prof. Salehi was an Associate Editor for Optical CDMA of the IEEE Transactions on Communications, since 2001 to 2012. He is among the 250 preeminent and most influential researchers worldwide in the Institute for Scientific Information (ISI) Highly Cited in the Computer-Science Category.